

---

# ON ANALYZING DELAY TIMES OF KINEMATIC OPTICAL MEASURING SYSTEMS WITH QUATERNION-ALGEBRA

*Claudia Depenthal*  
*Geodetic Institute, University of Karlsruhe*  
*Email: depenthal@gik.uka.de*

**Abstract:** Existing delay times in kinematic optical measuring systems will lead to deviations in spatiotemporal positioning. A time-referenced 4D test- and calibration system, existing by a rotating arm, will be used to the determination of the delay times. The modeling for the determination of the delay times is based on quaternion-algebra. The fundamental idea of modeling is equivalent to the fact that every test item's measurand, which is measured at a particular time, can be assigned to an explicit spatiotemporal known position. In this respect some results of lasertracker delay time determinations will be shown.

## 1. Introduction

Kinematic optical measuring systems such as lasertracker, robotic-tacheometer or iGPS are designed for space-time position determination of moving object points. These kind of measuring systems are multi-sensor systems and for a spatiotemporal positioning all involved sensors have to be synchronized. In fact there is a difference between the measured spatiotemporal position and the theoretical position. This difference is caused by the existence of delay times. In order to determine these delay times a time-referenced 4D test and calibration system was developed. The nominal trajectory is represented by a rotating arm and together with the time referencing every position is known in space and time. The modeling for the determination of the delay times is based on quaternion-Algebra.

## 2. 4D Test and Calibration System

### 2.1. Technical Realization

The time-referenced 4D test and calibration system consists of a tiltable rotating arm with an arm length of 2 m. At the end of the arm a prism or sensor can be fixed and a balance weight on the opposite end. A rotary direct drive with an integrated rotary encoder is used as prime mover of the rotating arm. The encoder has a resolution of 0.36" and the grating disk has a reference point, the so-called homepoint, for a defined orientation. After a calibration of the direct drive a measurement uncertainty for any angular position of  $U_{k=2} = \pm 4.2''$  is achieved [5]. The direct drive can produce velocities up to 10 m/s. However, up to now only 6 m/s at the arm's end has been used in default of a measuring system, which can follow objects moving with this high velocity.

The length of the rotating arm restricts the angular range of polar measurement systems. To enlarge the horizontal angle, a larger rotation has to be simulated for the measurement system.

---

This can be achieved by mounting the measurement system on a second rotary direct drive. In this way the measuring system performs the same rotation as the direct drive (c.f. Fig. 3, 4). This second direct drive is mounted on a very stable and heavy tripod. More details can be found in [3].

The main item of the test and calibration system are the direct drives and the control system with the real-time multi-axis servo motion controller PMAC (Programmable Multi-Axes Controller), which is used for the position and velocity control of the direct drives. The position-capture function latches the current encoder position at the time of an external event into a special register. The actual latching is executed in hardware, without the need for software intervention. This means that the only delays in a position capture are the hardware gate delays (less than 100 ns) thereby providing a very accurate capture function [3], [4].

## 2.2. Delay Time

In context with kinematic measurement systems the terms dead time and latency were often used. However, there are different definitions for these terms. For this reason and in combination with the time-referenced test and calibration system these terms are not applicable and the term delay time will be used instead. The delay time is defined as a time difference between a reference point and the execution time for every measurement value of a measurement system. The measurement value can be an angle or a distance for example. A clearly defined reference point is the time of the measurement request, because this is the time at which a complete measurement is expected. For every measurement request the reference time will be delivered by the control system. A certain time later an angle or distance will be measured and the delay time is now defined in relation to the measurement request [2]. In this way all delay times of a measurement system can be defined.

## 2.3. Time Referencing

The meaning of time referencing is, that specific procedures have to be assigned to a given time scale. For time referencing only real-time systems can be used. A system is said to be real-time, if the total correctness of the result of a real-time data processing depends not only upon its logical correctness, but also upon time in which it is performed [11]. A real-time system also has to guarantee a temporal deterministical behavior [10].

The time referencing is ensured with two different procedures. The first method of communication between the calibration system and a test item – measurement system – is an external trigger signal which is realized with a function generator using the rising edge of a rectangular signal as trigger. Fig. 1 shows a TTL (transistor-transistor-logic) circuit for a rising edge with a steepness of 1  $\mu$ s. Within the high level both, the measurement system ( $t_1$ ) and calibration system ( $t_2$ ), detect the trigger, but not at the same time. A time lag  $\Delta t$  within the referencing arise from the gate delay of both systems and can be calculated by the difference (1) of the trigger point, which are shifted by the gate delay

$$\Delta t = t_4 - t_3 \quad (1)$$

The gate delay of a measurement system is rarely known. The gate delay of the calibration system is less than 100 ns [2]. The reference point for the delay time determination is the trigger point detected by the calibration system.

The other method of communication is a serial interface. The communication is made up of request and reply in terms of the data item. The trailing edge of the start bit of the data item

will be captured and at the same time a trigger signal must be send to PMAC. To realize this in real-time a FPGA-modul (Field Programmable Gate Array) with a resolution of 25 ns is used. Fig. 2 shows the time referencing for an assumed data transfer rate of 19200 baud. The period between two trailing edges constitutes 103  $\mu\text{s}$ , so that the trailing edge of the start bit must be captured within this period. The same procedure can be done with the reply of the test item. In this way for every start bit of the request and reply a spatiotemporal position is known. The reference point for the delay time determination is the start bit of the request under considering of the known length of the data item [2].

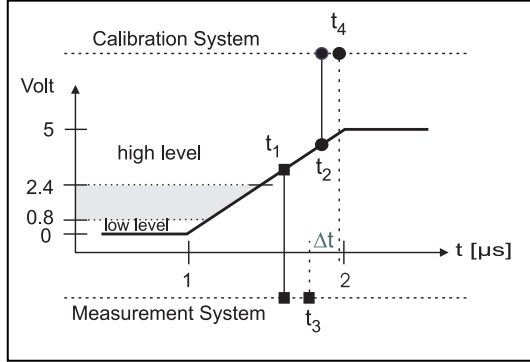


Figure 1: Time referencing with external trigger

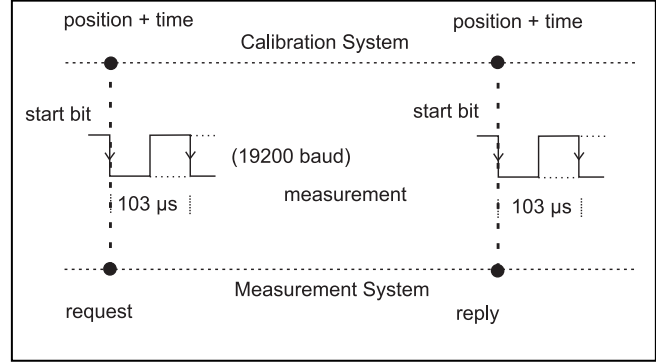


Figure 2: Time referencing with serial interface

### 3. Modeling

The test and calibration system can assign an exactly defined rotation angle in respect of the so-called homepoint and the associated time for the spatiotemporal position of a prism or sensor on the rotating arm. The aim of modeling is now the determination of the delay time for every measurand of a test item. Kinematic measurements are characterized by non-repeatable measurements and therefore the kinematic model must bear as unique unknown the delay time of the measurand. If the measurand itself is expressed as a function of the delay time, then the solution can be find e.g. by the Newton Iteration. To reach this aim the modeling is developed on quaternion-based rotations. The advantage of using quaternions is the efficient concatenation of multiple rotations and that only one rotation axis with one rotation angle will be used in the trigonometric form.

For all developed models a co-ordinate transformation must be executed to combine the co-ordinate system of the rotating arm with the co-ordinate system of the test item. This transformation will be calculated using quaternions also. The algorithm based on [7] and is also described in [3].

#### 3.1. Quaternion-Algebra

The theory of quaternions is given, for example, in [8] and therefore this subsection is only a short review about some of the basics.

A quaternion may be regarded as 4-tupel of real numbers, that is, as an element of  $\mathfrak{R}^4$ . A quaternion is defined as the sum

$$q = q_0 + \mathbf{q} = q_0 + iq_x + jq_y + kq_z . \quad (2)$$

In this sum  $q_0$  is called the scalar part and  $\mathbf{q}$  the vector part of the quaternion. The scalars  $q_0$ ,  $q_x$ ,  $q_y$  and  $q_z$  are called the components of the quaternion. Quaternions have their own algebra and the non-commutative multiplication of two quaternions  $p$  and  $q$  are given in (3).

$$pq = p_0q_0 - \mathbf{p} \cdot \mathbf{q} + p_0\mathbf{q} + q_0\mathbf{p} + \mathbf{p} \times \mathbf{q} \quad (3)$$

For a rotation in  $\mathfrak{R}^3$  the quaternion has to be a unit quaternion. The triple product (4) of the quaternion  $q$ , the complex conjugate quaternion  $q^*$  and the pure quaternion  $p$  ( $p = (0, \mathbf{p})$ ,  $\mathbf{p} \in \mathfrak{R}^3$ ) delivers as result a pure quaternion  $w$

$$w = qpq^* \quad (4)$$

(4) can be summarized in the matrix  $Q$  (6) – with the quaternion terms of  $q$  – and the multiplication with vector  $\mathbf{p} \in \mathfrak{R}^3$  results directly the vector  $\mathbf{w} \in \mathfrak{R}^3$ .

$$\mathbf{w} = Q\mathbf{p} \quad (5)$$

$$Q = \begin{pmatrix} 2q_0^2 - 1 + 2q_x^2 & 2q_xq_y - 2q_0q_z & 2q_xq_z + 2q_0q_y \\ 2q_xq_y + 2q_0q_z & 2q_0^2 - 1 + 2q_y^2 & 2q_yq_z - 2q_0q_x \\ 2q_xq_z - 2q_0q_y & 2q_yq_z + 2q_0q_x & 2q_0^2 - 1 + 2q_z^2 \end{pmatrix} \quad (6)$$

For any unit quaternion (2) the components can be expressed by

$$q_0 = \cos\left(\frac{\theta}{2}\right) \quad \mathbf{q} = \mathbf{u} \sin\left(\frac{\theta}{2}\right), \quad (7)$$

with  $\theta$  as rotation angle and  $\mathbf{u}$  as unit vector in the direction of  $\mathbf{q}$ . The triple product (4) may be interpreted geometrically as a rotation of the vector  $\mathbf{p}$  by an angle  $\theta$ , around  $\mathbf{q}$  as the rotation axis, to the new position of the vector  $\mathbf{w}$ .

### 3.2. Modeling for Polar Measuring Systems

If the test item is a polar measurement system, the resulting trajectory can consist of one rotation by the rotating arm, or of two rotations (additional rotation of the second direct drive under the test item). The development of both models starts in the rotating arm system with the starting point – the homepoint –  $\mathbf{p}_{D,1} = (r, 0, 0)^T$ , with  $r$  as known radius of the rotating arm (Fig 3). The x-axis and y-axis of the rotating arm system always lie in the rotating arm plane and the z-axis is taken to be planar to this plane.

#### 3.2.1. Polar modeling with one rotation

In this model the test item follows only the rotating arm (Fig. 3). The rotation axis for the first quaternion  $q_1$  (8) is equivalent to the z-axis of the rotating arm system. In this case  $q_1$  is already a unit quaternion. The rotation angle will be replaced by the relation of angular velocity  $\omega_D$  and time  $t$ . Due to the control system the angular velocity is known for every arm position and  $t$  can be used as the unknown delay time or it is the time for a known position.

$$q_1 = \left( \cos\left(\frac{t\omega_D}{2}\right), \begin{pmatrix} 0 \\ 0 \\ 1 \end{pmatrix} \sin\left(\frac{t\omega_D}{2}\right) \right) \quad (8)$$

For a new position  $\mathbf{p}_{D,2}$  in relation to the homepoint the triple product (4) will be used and with (8) and  $p_{D,1}$  as a pure quaternion, the result of (9) is also a pure quaternion

$$p_{D,2} = q_1 p_{D,1} q_1^* \quad (9)$$

In this way all positions on the rotating arm can be defined.

The next step is the transformation from the rotating arm system to the test item system. With the co-ordinate transformation, described in [7] or [3], the quaternions  $q_R$  and  $p_{tr}$  are determined for the rotation and translation between both co-ordinate systems. The result of the co-ordinate transformation for (9) is the same position, but now in the test item co-ordinate system

$$p_{P,2} = q_R p_{D,2} q_R^* + p_{tr} = q_R q_1 p_{D,1} q_1^* q_R^* + p_{tr} = q_R q_1 p_{D,1} (q_R q_1)^* + p_{tr} \quad (10)$$

The quaternion  $p_{P,2}$  is a pure quaternion and can be directly assigned as a vector  $\mathbf{p}_{P,2}$  in  $\mathfrak{R}^3$ . In (10) the catenation of quaternions is evident and both quaternions ( $q_R, q_1$ ) can be summarized in a matrix  $Q$  like (6). With (5) the vector  $\mathbf{p}_{P,2}$  has then the following form

$$\mathbf{p}_{P,2} = \begin{pmatrix} (2(q_{R,0}q_0 - q_{R,z}q_z)^2 - 1 + (q_{R,x}q_0 + q_{R,y}q_z)^2)r + p_{tr,x} \\ (2(q_{R,x}q_0 + q_{R,y}q_z)(q_{R,y}q_0 - q_{R,x}q_z) + 2(q_{R,0}q_0 - q_{R,z}q_z)(q_{R,z}q_0 + q_{R,0}q_z))r + p_{tr,y} \\ (2(q_{R,x}q_0 + q_{R,y}q_z)(q_{R,z}q_0 + q_{R,0}q_z) - 2(q_{R,0}q_0 - q_{R,z}q_z)(q_{R,y}q_0 - q_{R,x}q_z))r + p_{tr,z} \end{pmatrix} \quad (11)$$

and the only unknown is the time  $t$  in the terms  $q_0$  and  $q_z$  from (8) (cf. (2)).

Every measured position to the rotating arm from the test item can be expressed by (11). A single measurand, like angle or distance, can be calculated and now expressed as a function of the time  $t$ , which is the unknown delay time. The non-linear equations of the measurand cannot be solved analytical, but must be solved numerically e.g. by Newton's method. This iterative solution follows from the definition of recursion of Newton iteration. The algorithm is described in [2], [3]. The required initial value for the delay time determination delivers the time of the reference point for every measured position (cf. 2.3).

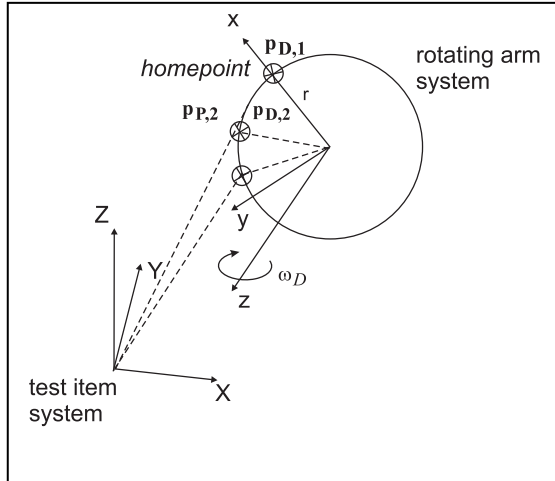


Figure 3: one rotation; rotating arm

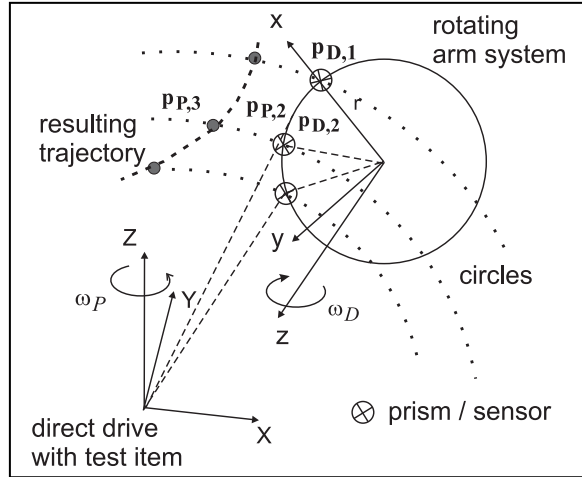


Figure 4: two rotations; rotating arm and test item

### 3.2.2. Polar modeling with two rotations

A second rotation results from the direct drive under the test item. If the test item has locked a prism or sensor and the second direct drive starts with rotation, the test item must countersteer to track the prism or sensor. The test item is then the center of a circle, with the measured distance as radius (Fig. 4). If at the same time the rotating arm starts with a rotation, then for every new position the circle's radius varies. The resulting trajectory depends on the angular

velocity of both direct drives and the arrangement of the tiltable rotating arm. The formation is neither a circle of the rotating arm nor a circle with the test item as center [3], [4].

For the second rotation of the test item a further quaternion  $q_2$  (12) will be used, with the Z-axis of the test item system as rotation axis and  $\omega_P$  as angular velocity. The time  $t$  is the same time like that of the quaternion  $q_1$ .

$$q_2 = \left( \cos\left(\frac{t\omega_P}{2}\right), \begin{pmatrix} 0 \\ 0 \\ 1 \end{pmatrix} \sin\left(\frac{t\omega_P}{2}\right) \right) \quad (12)$$

The starting point is as before the homepoint  $p_{D,1}$  as a pure quaternion. With (9) the first rotation by the rotating arm is described. Then the transformation in the test item system with the quaternions  $q_R$  and  $q_{tr}$  (10) follows. Until now it is the same procedure as if there is only one rotation. In the same time whereas the arm has rotated, the second direct drive under the test item rotates and the pure quaternion  $p_{P,2}$  will be rotated by the unit quaternion  $q_2$  to the new pure quaternion  $p_{P,3}$

$$p_{P,3} = q_2 p_{P,2} q_2^* = q_2 (q_R q_1 p_{D,1} q_1^* q_R^* + p_{tr}) q_2^* = q_2 q_R q_1 p_{D,1} (q_2 q_R q_1)^* + q_2 p_{tr} q_2^* . \quad (13)$$

The quaternion  $q_2$ ,  $q_R$ ,  $q_1$  can be summarized by piecewise multiplication e.g. in a new quaternion  $q_3$  and then with (6) a matrix  $Q_3$  can be designed. With the quaternion  $q_2$  as matrix  $Q_2$  equation (13) can be simplified as follows

$$\mathbf{p}_{P,3} = Q_3 \mathbf{p}_{D,1} + Q_2 \mathbf{p}_{tr} , \quad (14)$$

whereas  $\mathbf{p}_{P,3}$  is directly the spatiotemporal vector of the resulting trajectory. Every single measurand of the test item can be calculated by (14) and the only unknown in this non-linear equation is the delay time  $t$ . By the Newton iteration and the reference time as start value the delay time can be determined.

### 3.3. Modeling for Angular Measuring Systems

A spatiotemporal co-ordinate based on solely angular measuring can be determined by spatial intersection. A measuring system which based on solely angular measuring is e.g. the iGPS. This measuring system is described in [6], [1]. For the co-ordinate determination at least two test item position points are known and typically four measurands are used. For the modeling of a spatial intersection a vector model offers itself as an intersection of two skew straight lines. More details about this are given in [3].

For the delay time determination every measurand of the test item must correspond to a spatiotemporal position on the rotating arm. Then the measurand, e.g. an elevation, can be expressed as a function of the delay time. The first position of the test item is equivalent to the point of origin for the test item co-ordinate system. In this way it is the same as if a polar measurement system will be used. For the co-ordinate transformation the quaternion  $q_r$  and  $p_{tr}$  must be calculated and then the formal equation (10) can be used. From (11) both angles on this test item point are calculated and with the Newton iteration a delay time is determined.

If the test item's co-ordinate system is arranged in this way, that the second test item point coincide with the X-axis, then both points differ by a vector  $\mathbf{p}_{base}$

$$\mathbf{p}_{base} = (s_{1,2} \quad 0 \quad h_{1,2})^T , \quad (15)$$

---

with  $s_{1,2}$  as distance and  $h_{1,2}$  as height between both test item points. The position on the rotating arm  $\mathbf{p}_{P,2B}$  from the second test item point is built as follows

$$\mathbf{p}_{P,2B} = \mathbf{p}_{P,2} - \mathbf{p}_{\text{base}} \quad (16)$$

From (16) again both angles and the delay time is calculated for the second test item position. More detailed formulas are given in [3]. In this case an ideal spatial intersection can be assumed, because only the measurands of the test item are used for the delay time determination.

### 3.4. Measurement Uncertainty

In order to make a statement about the quality of the delay times, a measurement uncertainty must be determined for every discrete delay time. The measurement uncertainty will be deduced from the static determined co-ordinate transformation. The residuals of this transformation include the measurement uncertainty of the rotating arm, as well as the measurement uncertainty of the test item. From these residuals for every measurand of the test item a standard uncertainty is determined which in the following will be assumed as a boundary value for the determination of measurement uncertainty for delay times.

Co-ordinates in the rotating arm system are calculated with an increment of 1 ms for every rotating arm velocity. Afterwards the co-ordinates will be transformed into the test item system and translated in measurands of the test item. In this way measurement values with a temporal distance of 1 ms are given for every measurand. The result of the differences between these values is a sinusoidal function because of the circular trajectory. For every rotating arm position a function value can be calculated and then the measurement uncertainty of the delay time is given by the quotient of the boundary value and a function value. In order to increase the confidence interval of the measurement uncertainty a multiplication by a factor  $k = 2$  gives the expanded measurement uncertainty ( $U_{k=2}$ ) of every delay time. More details are given in [3]. Due to the characteristics of the direct drive, the quality of the co-ordinate transformation between the test item and the test equipment was increased by using a very slow rotation of the rotating arm instead a static measurement.

## 4. Exemplary Measuring Results

The delay time determination for the measurands of a robotic-tacheometer is presented in [3] and indicates precise examination results. The measurements with a lasertracker illustrate the high quality of the test and calibration system. Therefore, delay times for the lasertracker were derived by self-calibrating methods, such as changing the rotation direction of the rotating arm and/or varying the test item distance. These methods enable to separate effects of the test item and the test equipment.

The following exemplary results are executed with a Leica LTD500 lasertracker and with a Leica Absolute Tracker AT901-MR with TCAM. The rotating arm is arranged in a vertical position. The time referencing is realized with a function generator as external trigger, with a clock frequency of 40 Hz. For the co-ordinate transformation the measurement is executed by an angular velocity of 5°/s for the rotating arm. The test item was positioned in the rotating axis at a distance of about 1.4 m. A first impression of measurement results delivers a 3D circle fitting using the least-squares method. For AT901 without TCAM Fig. 5 shows the planar deviations (perpendicular to the plane of the circle) and Fig. 6 the radial deviations with an angular velocity  $\omega_D$  of 190°/s and 23 rounds. This corresponds to a maximum angular

velocity  $\omega_{T_{max}}$  of the lasertracker head of 3.8 m/s @ 1.4 m and 2.7 rad/s, respectively, which is inside of the specification (“tracking speed lateral < 4 m/s” [9]). The changes of moving direction of the lasertracker head are at the rotating arm position of  $-117^\circ$  and  $-297^\circ$ . The planar deviations by a velocity of  $5^\circ/s$  are less than  $\pm 50 \mu\text{m}$  and the radial deviations remain nearly in the same range. In this way both results show a stable behavior of the rotating arm at higher velocities.

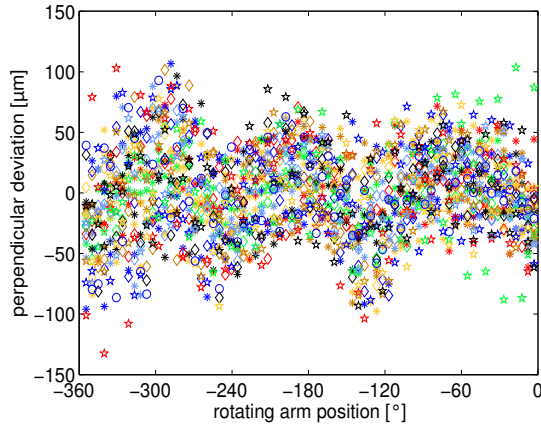


Figure 5: planar deviation at  $\omega_D = 190^\circ/s$ , AT901 @  $\omega_{T_{max}} = 2.7 \text{ rad/s}$

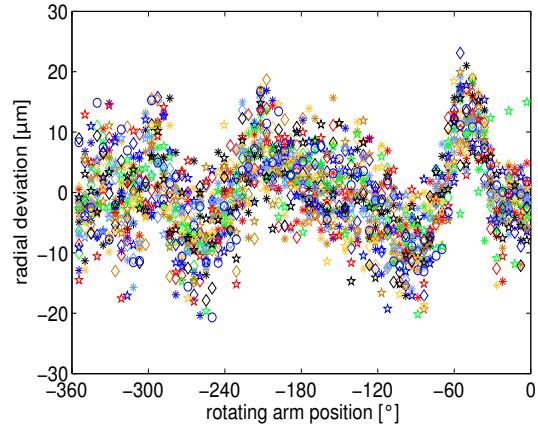


Figure 6: radial deviation at  $\omega_D = 190^\circ/s$ , AT901 @  $\omega_{T_{max}} = 2.7 \text{ rad/s}$

After the co-ordinates of the lasertracker are transformed into the rotating arm system, the angles in relation to the homepoint (rotating arm position =  $0^\circ$ ) are calculated. In the best case these angles are, within the accuracy of the calibration system and test item, the same as the time-referenced angles of the PMAC-encoder. Fig 7 shows the differences between both angles, calculated as a tangential distance for the AT901 without TCAM, again at an angular velocity  $\omega_D = 190^\circ/s$ . At the angular velocity of  $5^\circ/s$  the range is between  $\pm 25 \mu\text{m}$ .

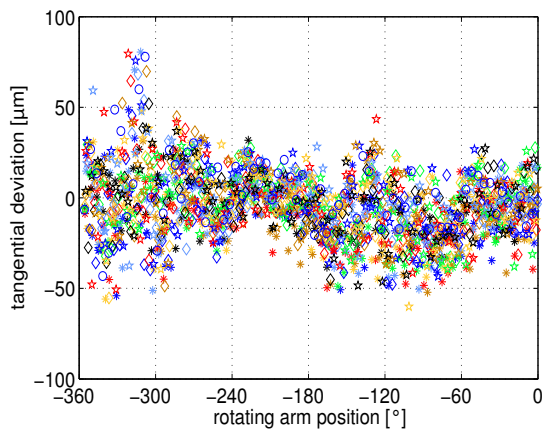


Figure 7: tangential deviation at  $\omega_D = 190^\circ/s$ , AT901 w/o TCAM @  $\omega_{T_{max}} = 2.7 \text{ rad/s}$

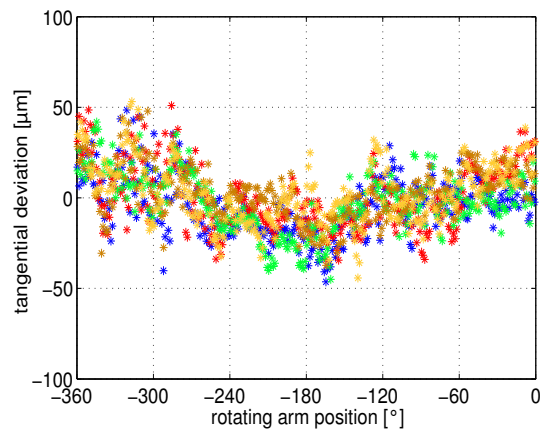


Figure 8: tangential deviation at  $\omega_D = 50^\circ/s$ , AT901 with TCAM @  $\omega_{T_{max}} = 1.4 \text{ rad/s}$

With lasertracker remained in the same position and the TCAM mounted, the angular velocity of the rotating arm was reduced to  $\omega_D = 50^\circ/s$  (corresponding to  $\omega_{T_{max}} = 1.4 \text{ rad/s}$  and 1 m/s @ 1.4 m) because of the specification with TCAM (“tracking speed lateral < 1 m/s” [9]). Fig. 8 shows the tangential deviations. With respect to the moving direction of the lasertracker head, the negative and positive values show a more clearly trend with the TCAM mounted

than without TCAM. Measurements beyond the specification intensify this trend, but should be used only for verification. A change of the rotation direction of the rotating arm gives the same results, so effects of the test equipment can be excluded widely.

Delay times were determined for the lasertracker with and without TCAM including their uncertainties. Due to geometrical restrictions, there are angular ranges, which are not suited to derive delay times (see Fig. 9 and 10, bottom). Note, that with decreasing angular velocity, the uncertainty of the delay time increases. Fig. 9 (top) shows the delay time for the vertical angle of the lasertracker without TCAM. The range is less than  $\pm 0.03$  ms and corresponds to the interpolation interval of the lasertracker. The measurement uncertainty is similar to the dimension of the delay time. Fig. 10 shows the delay time for the experiment with the TCAM mounted, and therefore the angular velocity  $\omega_D = 50^\circ/\text{s}$ . The TCAM seems to produce larger delay times, but note, that the measurement uncertainty due to the reduced angular velocity increases also. The delay time determination for the horizontal angle shows similar results. The LTD500 exhibits under the same conditions nearly the same results as AT901 without TCAM.

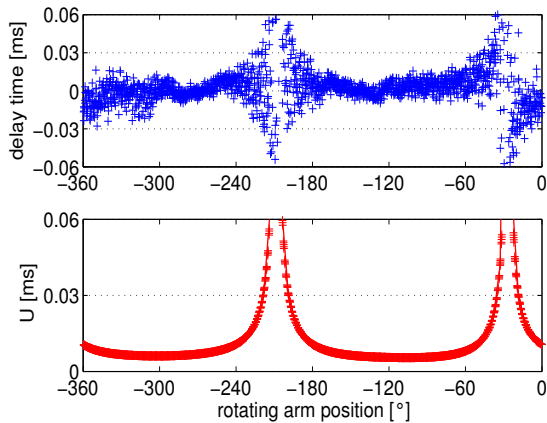


Figure 9: delay time vertical angle (top),  $\omega_D = 190^\circ/\text{s}$ , AT901 w/o TCAM

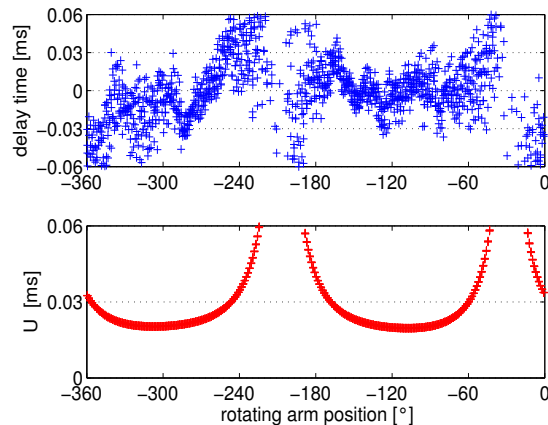


Figure 10: delay time vertical angle (top),  $\omega_D = 50^\circ/\text{s}$ , AT901 with TCAM

## 5. Conclusion

By using kinematic optical measuring systems delay times will lead to deviations in spatiotemporal position determination of moving objects. For the determination of delay times a time-referenced 4D test and calibration system and an adequate modeling were developed. The modeling bases on the theory of quaternions. The aim of modeling is the determination of the delay time for every measurand of a test item. Therefore the measurand itself must be expressed as a function of the delay time. The lasertracker test measurements show the high quality of the test and calibration system and the successful modeling. First investigations show that both lasertrackers (LTD500, AT901) works fine within its operation range. To verify these results a more detailed modeling, which include the internal mechanism will be useful.

## References

- [1] Depenthal, C.; Schwendemmann, J.: iGPS – a New System for Static and Kinematic Measurements. 9<sup>th</sup> Conference on Optical 3D Measurement Techniques, 2009

- 
- [2] Depenthal, C.: Quaternion-Based Delay time determination for kinematic optical measuring systems. Eurocon 2009, International IEEE Conference, Saint-Petersburg, Russia, 2009 (in print)
  - [3] Depenthal, C.: Entwicklung eines zeitreferenzierten 4-D-Kalibrier- und Prüfsystems für kinematische optische Messsysteme. Deutsche Geodätische Kommission (DGK), Reihe C, Heft-Nr. 627, 2009
  - [4] Depenthal, C.: A Time-referenced 4D Calibration System for Kinematic Optical Measuring Systems. Proceedings of 1st International Conference on Machine Control & Guidance, 24-26 June 2008, Zurich, Switzerland
  - [5] Depenthal, C.: Automatisierte Kalibrierung von Richtungsmesssystemen in rotativen Direktantrieben. AVN 8/9/2006, p. 305-309, 2006
  - [6] Hedges, T., Takagi, H., Pratt, T., Sobel, M. J.: Position Measurement System and Method using Cone Math Calibration. US Patent No. US 6,535,282 B2, 2003
  - [7] Horn, B. K. P.: Closed-form solution of absolute orientation using unit quaternions. Journal of the Optical Society of America A, Vol.4, No.4 p. 629-642, 1987
  - [8] Kuipers, J. B.: Quaternions and Rotation Sequences - A Primer with Applications to Orbits, Aerospace, and Virtual Reality. Princeton University Press, 1999
  - [9] Leica Geosystems: PCMM System Specifications, Leica Absolute Tracker and Leica T-Products. [www.leica-geosystems.com/metrology](http://www.leica-geosystems.com/metrology), 2008
  - [10] Mächtel, M.: Entstehung von Latenzzeiten in Betriebssystemen und Methoden zur Messtechnischen Erfassung. Fortschritt-Berichte VDI Reihe 8 Nr. 808, VDI-Verlag Düsseldorf, 2000
  - [11] Wörn, H.; Bringschulte, U.: Echtzeitsysteme. Springer-Verlag Berlin Heidelberg, 2005

published in:

Grün, A. / Kahmen, H. (eds.), Optical 3-D Measurement Techniques IX, Vol. I, Vienna / Austria, Jul. 1-3, 2009, pp. 105-114, 2009.